WEICHENG REN
DENGPAN QIAO
JUN JIE BA
and
GUANGTAO LI

# Relationship between the height of the compression region and the underflow concentration of a vertical silo with consecutive discharge

*A continuous tailings discharge model is proposed to solve the problems of high fluctuations in underflow concentration and relatively low, unstable actual discharge concentration in vertical tailing silos. A mathematical model for continuous tailing discharge was derived based on mass balance equation. A partial differential equation related to the height of the tailing silo in the compression area and tailing slurry concentration was also obtained. Results of the centrifuge and intermittent sedimentation tests show that the effective solid stress equation and solid flux equation correspond with each other. Thus, the relationship between the height of the compression region and the underflow concentration is exponential; subsequently, the exponential equation can be fitted.*

*Keywords: Consecutive underflow, solid flux density function, effective solid stress, dynamic sedimentation.*

## 1. Introduction

Vertical tailing silos are a type of main structure used for hydraulic filling. It is usually made of a cylinder 8-10 m in diameter and 18-20 m in height, and a half-sphere or cone with a certain angle at the bottom. Multiple tailing silos have an underflow alternate to ensure the balance between mining and filling in a mine. Given that tailing silos have an underflow, multiple tailing silos must be built to ensure that tailings feeding and settlement have sufficient time to happen. The secondary recovery of mortar overflow with mortar volume concentration inevitably ranges between 7% and 12% of the overflow. The tailings standing at the bottom of the cone for a long time, combined with increasing pressure, results in a highly dense accumulation of tailings, such that underflow is required with high-pressure air and water. The fluctuation of underflow concentration is large, restricting the increase of filling slurry concentration, and then causing the high consumption of cement for filling. The calibration data (more than 10%) has been confirmed by a project group. Thus, the cemented filling quality and the high cost of filling cannot be guaranteed.

High-density tailings and a high settlement container of the vertical tailing silo with a smaller diameter can achieve a good effect of continuous concentration. Therefore, a continuous high-density discharge model is proposed to target existing problems in using the present gravity sedimentation model of vertical tailing silos. Such problems include, the need for a second-time pulping of alternative tailings discharge with the simultaneous action of multiple silos, and tailings discharge from the bottom flow, as well as the high range of density fluctuations and difficulty in controlling such fluctuations during the tailings discharge process [1, 2].

## 2. Mathematical model of the consecutive underflow

A vertical tailing silo maintains a steady state when it has consecutive underflow.

A dynamic equilibrium process would then exist on the condition of temporal affecting factor and meet the following condition:

Feeding (tailings+ water) = Overflow (water) + Underflow (tailings+ water).

The volumetric solids concentration $\phi$ is constant across each horizontal cross-section, i.e., $\phi = \phi(x, t)$. Then, the conservation of mass equation for solids is given by:

$$S(\mathrm{x})\frac{\partial \phi}{\partial t} + \frac{\partial}{\partial x}\left(S(\mathrm{x})\phi\, \mathrm{v}_s\right) = 0 \qquad \ldots \quad (1)$$

where $t$ is time, and $v$ is the solid-phase velocity. The analogue conservation equation for the fluid reads as follows:

$$-S(\mathrm{x})\frac{\partial \phi}{\partial t} + \frac{\partial}{\partial x}\left(S(\mathrm{x})(1-\phi)\, \mathrm{v}_f\right) = 0 \qquad \ldots \quad (2)$$

Messrs. Weicheng Ren, Dengpan Qiao, Jun Jie Ba and Guangtao Li, Faculty of land Resource Engineering, Kunming University of Science and Technology, Kunming, Yunnan, 650 093, and Guangtao Li, Dahongshan Copper Mining, Yuxi Mining Co., Ltd., Xuxi, Yunnan, 653 100, China. Email: qiaodengpan690821@126.com

where $v_f$ is the fluid-phase velocity. The mixture flux, which is the volume average flow velocity appropriately weighted with the cross-sectional area at height $x$, is given by:

$$Q(\mathrm{x,t}) = \mathrm{S(x)}\left(\phi\, \mathrm{v}_s + (1-\phi)\, \mathrm{v}_f\right) \quad \ldots \quad (3)$$

The sum of Eqs. (1) and (2) produces the continuity equation of the mixture:

$$\frac{\partial}{\partial x} Q(\mathrm{x,t}) = 0 \quad \ldots \quad (4)$$

Equation (4) implies that $Q(x, t)$ is constant as a function of $x$. Given that this quantity suffers no jump across a discontinuity of $\phi$, the following equation is obtained:

$$Q(x,\ \ t) = Q_D(t) \quad \ldots \quad (5)$$

Equation (5) is equivalent to one of the mass balance equations. It can be used to replace the fluid mass balance [Eq. (2)] and rewrite the solid balance [Eq. (1)] in terms of the flow rate $Q_D(t)$ and the solid–fluid relative velocity or slip velocity $v_r = v_s$-$v_f$, for which a constitutive equation will be formulated. As such:

$$S(x)\phi v_s = S(x)\left[\left(\phi v_s + (1-\phi)v_f\right)\phi + \phi(1-\phi)\left(v_s - v_f\right)\right] = Q(t)\phi + S(x)\phi(1-\phi)v_r \quad \ldots \quad (6)$$

The Eq. (6) can be written as follows from Eq. (1):

$$S(\mathrm{x})\frac{\partial \phi}{\partial t} + \frac{\partial}{\partial x}\left[Q(\mathrm{t})\phi + \mathrm{S(x)}\phi(1-\phi)\,\mathrm{v_r}\right] = 0 \quad \ldots \quad (7)$$

The well-known kinematic sedimentation theory by Kynch (1952) is based on the assumption that the solid-fluid relative velocity or slip velocity $v_r$ is a function of the local solids concentration $\phi$ only, that is, $v_r = v_r(\phi)$ [3]. Slip velocity is usually expressed in terms of the Kynch batch flux density function $f_{bk}$. In the framework of kinematic theory, slip velocity is expressed as:

$$v_r = \frac{f_{bk}(\phi)}{\phi(1-\phi)} \quad \ldots \quad (8)$$

Thus, Eq. (7) can take the form:

$$S(\mathrm{x})\frac{\partial \phi}{\partial t} + \frac{\partial}{\partial x}\left[Q(\mathrm{t})\phi + \mathrm{S(x)\,f_{bk}}(\phi)\right] = 0 \quad \ldots \quad (9)$$

The model is provided by the phenomenological theory of sedimentation [4], which is based on the mass and linear momentum balance equations for solid and fluid components. By introducing constitutive assumptions, performing a dimensional analysis, and considering only a one space dimension, we find that the theory leads to the following equation for relative velocity $v_r$, which plays the role of one of the linear momentum balances:

$$v_r = \frac{f_{bk}(\phi)}{\phi(1-\phi)}\left(1 + \frac{\sigma_e'(\phi)}{\Delta\rho g \phi}\phi_x\right) \quad \ldots \quad (10)$$

where: $\Delta\rho$>0 denotes the solid-fluid density difference, g is the acceleration of gravity, and $\sigma_c(\phi)$ is the derivative of the effective solid stress function $\sigma_c(\phi)$ [5-7].

Inserting Eq.(10) into Eq.(7) leads to the following definition:

$$a(\phi) = \frac{f_{bk}(\phi)\sigma_e'(\phi)}{\Delta\rho g \phi},\ A(\phi) = \int_0^{\phi} a(\mathrm{s})\,\mathrm{ds} \quad \ldots \quad (11)$$

through which the field equation can be obtained:

$$S(\mathrm{x})\frac{\partial \phi}{\partial t} + \frac{\partial}{\partial x}\left(Q(t)\phi + S(\mathrm{x})\,\mathrm{f_{bk}}(\phi)\right) = \frac{\partial}{\partial x}\left[S(\mathrm{x})\frac{\partial A(\phi)}{\partial x}\right] \quad \ldots \quad (12)$$

With the condition of a time constant, Eq.(12) is simplified to:

$$\frac{d}{dx}(\mathrm{q}\,\phi + \mathrm{f}_{bk}(\phi)) = \frac{d^2 A(\phi)}{dx^2} \quad \ldots \quad (13)$$

Such solutions satisfy the ordinary differential equation, which Eq. (12) indicates is stationary, i.e., independent of time.

$$Q_D\phi(\mathrm{x}) + \mathrm{S(x)\,f_{bk}}(\phi(\mathrm{x})) = \mathrm{S(x)}\frac{dA(\phi)}{dx} + C \quad \ldots \quad (14)$$

where $C$ is a constant of integration, and $C = Q_D\phi_D$. Inserting $C$ into Eq.(14), the following equation can be obtained:

$$Q_D(\phi(\mathrm{x}) - \phi_{\mathrm{D}}) + \mathrm{S(x)\,f_{bk}}(\phi(\mathrm{x})) = \mathrm{S(x)}\frac{dA(\phi)}{dx} \quad \ldots \quad (15)$$

For the corresponding concentration profile $\phi = \phi(x)$, the concentration with respect to the independent variable $x$ is shown as the following equation:

$$\phi'(\mathrm{x}) = \frac{d\phi}{dx} = \frac{\Delta\rho g\phi(q(\phi - \phi_D) + \mathrm{f}_{bk}(\phi))}{f_{bk}(\phi)\sigma_e'(\phi)} \quad \ldots \quad (16)$$

## 3. Material and method

### 3.1 Material

The experimental raw material was tailings from the Dahongshan copper mine in Yunnan, China. The tailing density was 2.897 g/cm$^3$, which was measured by a pycnometer.

### 3.2 Methods

Solid flux density function and effective solid stress are important parts of the mathematical model of consecutive underflow in tailing silos. The solid flux density function determines the characteristics of solids settlement. Meanwhile, the effective solid stress determines the technological parameters, such as the largest concentration

and the height of the tailing silo compression area, and so on. Parameters $\alpha_1$ and $\alpha_2$ in the effective solid stress function ($\sigma_e(\phi)$) were obtained through centrifuge tests, while parameters $v_x$ and $n$ in the solid flux density function ($f_{bk}$) were obtained through sedimentation experiments. The different properties of materials resulted in different experimental parameters [8].

*(1) Effective solid stress measurement*

The effective solid stress was measured in the compression zone. Buscall and White suggested that effective solid stress, which is a function of volume fraction, can be obtained using Eq. 17 [9-11]:

$$\sigma_e(\phi) = \begin{cases} 0 & \phi \le \phi_c \\ \alpha_1 \exp(\alpha_2 \phi) & \phi > \phi_c \end{cases} \quad \text{... (17)}$$

where $\phi_c$ is the gel point that can be obtained according to the gel point measurement described in a later section, and $\alpha_1$ and $\alpha_2$ are constant parameters that can be obtained using experimental tests. Several effective solid stresses and corresponding solid volume fraction values were obtained through the experimental tests.

Gel point ($\phi_c$) is the solid volume fraction at the beginning of the compression zone. An indirect method for obtaining the gel point was used by Tiller and Khatib. This method is related to the batch-settling tests. For each settling test, the equilibrium height of the sediment bed ($h_c$) was determined, and the gel point ($\phi_c$) was calculated according to Eq. 18 [12]:

$$\phi_c = \frac{\phi_1 h_1}{h_c} \quad \text{... (18)}$$

Gel point ($\phi_c$) was 0.296 as calculated using Eq. (18), where $\phi_1$ and $h_1$ are the initial solid volume fraction and initial height of the suspension respectively for each settling test, and $h_c$ is the equilibrium height of the sediment bed that can be calculated from each batch-settling curve.

This method to estimate the effective solid stress using batch centrifuge experiments was carried out via a centrifuge 3–5 w (HENGNUO). The centrifuge tubes used in these measurements had a suspension volume of 15 ml and a diameter of 12 mm. Different rotational speeds in the range of 400–1700 rpm were used [13,14].

To calculate the effective solid stress measurement, batch centrifuge experiments were performed. For each test, the initial suspension height in the test tube ($h_0$), the initial solid volume fraction of the suspension ($\phi_0$), the centrifugal acceleration (g), and the final mud line height ($h_{eq}$) were determined, and the effective solid stress ($\sigma_c$) as well as solid volume fraction ($\phi$) were calculated. Details are shown in Table 1.

The experimental data were fitted to Eq. (17), and the fitted curve is shown in Fig.1.

The parameter values $\alpha_1$ = 5.18 and $\alpha_2$ = 14.42. Thus, Eq. (17) can be expressed as: $\sigma_e(\phi) = 5.18\exp(14.42*\phi)$ ($\phi > \phi_c$)

TABLE 1: RESULTS OF CENTRIFUGE TESTS

| Rotation speed/pm | RCF/g | $h_{eq}$/m | $\sigma_e$(f) | $\phi$/% |
|---|---|---|---|---|
| 400 | 19.68 | 0.035125 | 3484.90 | 0.4698 |
| 600 | 44.27 | 0.0335 | 7903.21 | 0.5174 |
| 800 | 78.71 | 0.03175 | 14169.22 | 0.5470 |
| 1000 | 122.98 | 0.02975 | 22352.02 | 0.5732 |
| 1200 | 177.09 | 0.028 | 32454.82 | 0.6120 |
| 1500 | 276.71 | 0.0275 | 50830.26 | 0.6319 |
| 1700 | 355.41 | 0.027 | 65442.26 | 0.6552 |

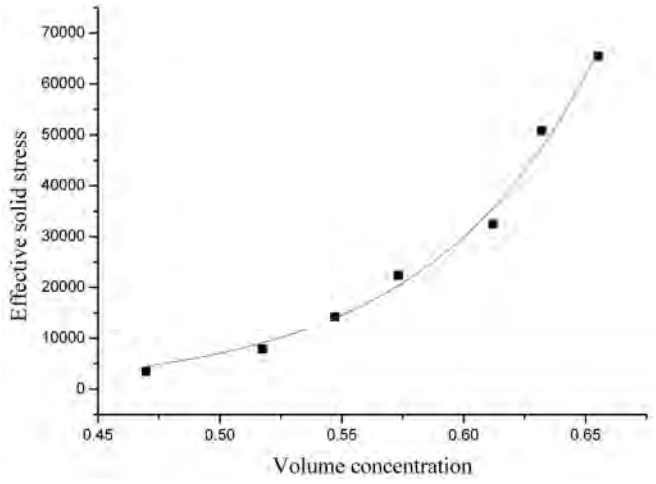


Fig.1 Experimental data obtained from batch centrifuge experiments and curve of the equation

*(2) Measurement of solid flux density function*

Solid flux is defined as follows. The solid quality of the unit surface is equivalent to the sedimentation rate multiplied by the sludge concentration per unit time. A typical example is attributed to Michaels and Bolger (1962) [15, 16]:

$$f_{bk}(\phi) = \begin{cases} v_\infty \phi (1 - \dfrac{\phi}{\phi_{\max}})^n & 0 < \phi < \phi_{\max} \\ 0 & \text{other} \end{cases} \quad \text{... (19)}$$

The mass concentrations of the six group mortars formed ranged from 15% to 40% solutions. The batch experiment of tailings was carried out respectively [17, 18]. The results are shown in Table 2.

TABLE 2: RESULTS OF TAILINGS SETTLING EXPERIMENT

| Volume concentration | Settling velocity (m/s) | Suspension concentration (kg/m$^3$) | Solid flux (kg/m$^2$*s) |
|---|---|---|---|
| 0.06 | 0.00048913 | 166.09 | 0.08124 |
| 0.08 | 0.00037371 | 229.67 | 0.08583 |
| 0.10 | 0.00026980 | 298.14 | 0.08044 |
| 0.13 | 0.00019538 | 372.10 | 0.0727 |
| 0.16 | 0.00013995 | 452.23 | 0.06329 |
| 0.19 | 0.00009677 | 539.34 | 0.05219 |

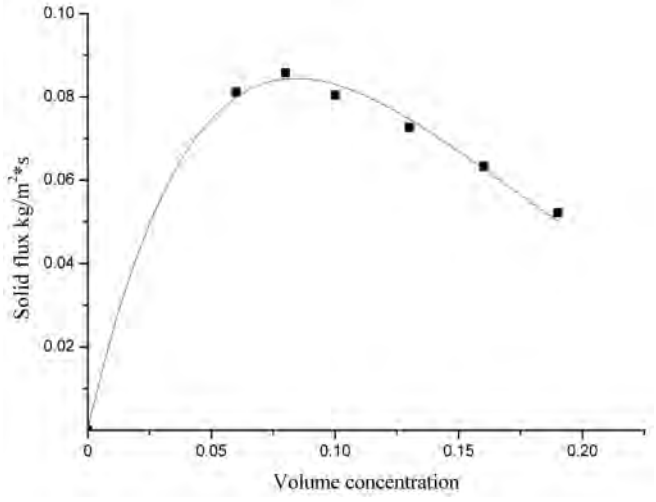


Fig.2 Fitting formula curve of solid flux density

The solid flux density function curves were plotted according to the batch experiment data. The abscissa is the volume concentration, and the ordinate is the solid flux density. The experimental data was fitted to Eq. (19), and the fitted curve is shown in Fig.2.

The parameter values $v_x$ = 2.61 and n = 10.86. Hence, Eq. (19) can be expressed as $f_{bk}(\phi)=2.61\phi\,(1-\phi)^{10.86}$

## 4. Relationship between the height of the compression region and the underflow concentration

Every 0.05 value from the underflow concentration ranges of 0.52 - 0.58 was substituted into the differential Equation (16). The relationship between the height of the compression region and the underflow concentration was solved using Matlab software. The calculation results are presented in Table 3.

Fig.3 shows that an exponential relationship can be established between the underflow concentration as the abscissa and the height of the compression region as the ordinate.

TABLE 3: VALUES OF THE CHANGE OF THE UNDERFLOW CONCENTRATION WITH THE HEIGHT OF THE COMPRESSION REGION

| Underflow concentration | Compression region height (m) |
|---|---|
| 0.52 | 7.51 |
| 0.525 | 8.08 |
| 0.53 | 8.69 |
| 0.535 | 9.36 |
| 0.54 | 10.07 |
| 0.545 | 10.83 |
| 0.55 | 11.66 |
| 0.555 | 12.54 |
| 0.56 | 13.5 |
| 0.565 | 14.54 |
| 0.57 | 15.65 |
| 0.575 | 16.86 |
| 0.58 | 18.16 |

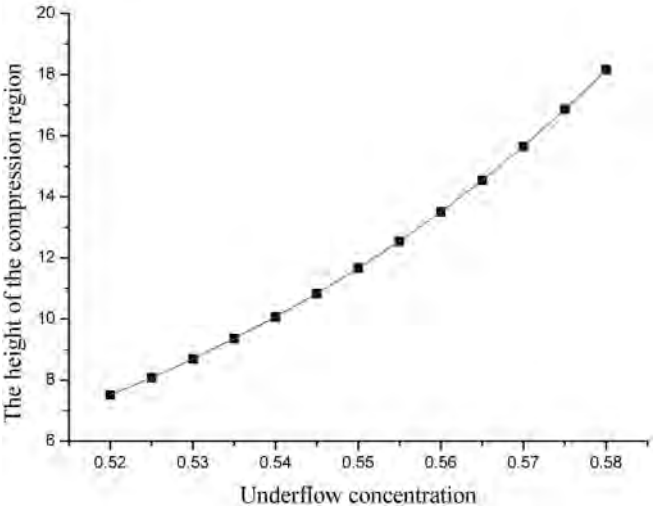


Fig.3 Fitting the formula curve of the change of the underflow concentration to the height of the compression region

The exponential equation $y = a+be^{cx}$ can be selected as the regression equation, and the values of the underflow concentration and the height of the compression region were substituted into the regression equation. The parameter values were $a$ = 0.25, $b$ = 0.00292, and $c$ = 15.03. Hence, the regression equation can be expressed as

$H = 0.25+0.00292e^{15.03Cv}$.

## 5. Conclusions

(1) A mathematical model for continuous tailing discharge is derived based on a mass balance equation. A partial differential equation, $\phi'(x)=\frac{d\phi}{dx}=\frac{\Delta\rho g\phi(q(\phi-\phi_D)+f_{bk}(\phi))}{f_{bk}(\phi)\sigma_e'(\phi)}$, related to the height of tailing silos in the compression area and the tailing slurry concentration is also obtained.

(2) Every 0.05 value from the underflow concentration ranges of 0.52 to 0.58 can be calculated by substituting these values into the continuous, highly concentrated, and stable discharge tailing model. Therefore, the height of the interface level between the tailings and water, achieves an exponential relationship when the tailings discharged by the tailing silo reach a dynamic balance. The corresponding relation of the underflow concentration and the height of the interface level between the tailings and water is obtained through regression of the relevant equations above.

## Acknowledgments

This work was financially supported by National Natural Science Foundation of China (51164016) and the Key Science and Technology Projects of Gansu Province (1203GKKDC003).

## References

1. Deb, S. D. (2000): "Analysis of real-time shield pressures for the evaluation of longwall ground control problems," *Journal of Mines Metals & Fuels*, vol. 48, pp. 230-236, 2000.
2. Ren, W. C. and Qiao, D. P. (2016): "Numerical Simulation of Particle-Phase Distribution Based on Tailings Slurry Filling of Silo," *Electronic Journal of Geotechnical Engineering*, no. 21.19, pp. 6515-6520, 2016.
3. Kynch, G. J. (1952): "A theory of sedimentation," *Transactions of the Faraday Society*, vol. 48, no. 2, pp. 166-176, 1952.
4. Burger, R., Wendland, W. L. and Concha, F. (2000): "Model equations for gravitational sedimentation–consolidation processes," *Zamm Journal of Applied Mathematics & Mechanics Zeitschrift Fur Angewandte Mathematik Und Mechanik*, vol. 80, no.2, pp. 79-92, 2000.
5. Burger, R. and Concha, F. (1988): "Mathematical model and numerical simulation of the settling of flocculated suspensions," *International Journal of Multiphase Flow*, vol. 24, no. 6, pp. 1005-1023, 1988.
6. Burger, R. and Concha, F. (2001): "Settling velocities of particulate systems: 12. Batch centrifugation of flocculated suspensions," *International Journal of Mineral Processing*, vol. 63, no. 3, pp. 115-145, 2001.
7. Burrger, R. and Karlsen, K. H. (2001): "On some upwind schemes for the phenomenological sedimentation–consolidation model," *Journal of Engineering Mathematics*, vol. 41, no. 2, pp. 145-166, 2001.
8. Burger, R. and Concha, F. (2001): "Phenomenological model of filtration processes: 1. Cake formation and expression," *Chemical Engineering Science*, vol. 56, no. 15, pp. 4537-4553, 2001.
9. Buscall, R. and White, L. R. (1987): "The consolidation of concentrated suspensions Part 1: The theory of sedimentation," *Journal of the Chemical Society: Faraday Transaction I*, vol. 83, pp. 873-891, 1987.
10. Carrillo, J. (1999): "Entropy Solutions for Nonlinear Degenerate Problems," *Archive for Rational Mechanics and Analysis*, vol. 147, no. 4, pp. 269-361, 1999.
11. Been, K. and Sills, G. C. (2015): "Self-weight consolidation of soft soils: an experimental and theoretical study," *Géotechnique*, vol. 31, no. 4, pp. 519-535, 2015.
12. Tiller, F. M. and Khatib, Z. (1983): "The theory of sediment volumes of compressible, particulate structures," *Journal of Colloidal and Interface Science*, vol. 100, no.1, pp. 56-67, 1983.
13. Green, M. D. and Boger, D. V. (1997): "Yielding of suspensions in compression," *Industrial & Engineering Chemistry Research*, vol. 36, no. 11, pp. 4984-4992, 1997.
14. Channell, G.. M. and Zukoski, C. F. (1997): "Shear and compressive rheology of aggregated alumina suspension," *AIChE Journal*, vol. 43, no. 7, pp. 1700-1708, 1997.
15. Xu, S. G. and Ba, J. J. (2016): "Predicting Strata Temperature Distribution from Drilling Fluid Temperature," *International Journal of Heat and Technology*, vol. 34, no. 2, pp. 345-352, 2016.
16. Richardson, J. F. and Zaki, W. N. (1954): "Sedimentation and fluidization: Part I," *Transactions of the Institution of Chemical Engineers*, vol. 32, pp. 35-53, 1954.
17. Michaels, A. S. and Bolger, J. C. (1966): "Settling rates and sediment volumes of flocculated Kaolin suspensions," *Industrial & Engineering Chemistry Fundamentals*, vol. 10, no. 1, pp. 24-33, 1966.
18. Madhu, B., Nagarajan, P. K. and Edwin, M. (2016): "Experimental investigations on conventional solar still with sand heat energy storage," *International Journal of Heat and Technology*, vol. 34, no. 4, pp. 597-603, 2016.


---

## GEOLOGICAL CONTROLS ON CBM ENRICHMENT AND ITS EXPLORATION TARGET OPTIMIZATION IN THE SOUTHEAST JUNGGAR BASIN, CHINA

*Continued from page 143*


24. Fu, H., Tang, D. Xu, H., Tao, S., Xu, T., Chen, B. and Yin, Z. (2016):" Abrupt changes in reservoir properties of low-rank coal and its control factors for methane adsorbability," *Energy & Fuels*, vol 30, no.3, pp. 2084-2094, 2016.
25. Sen, S., Das, N. and Mait, D. (2016): "Facies analysis and depositional model of late Permian Raniganj formation: Study from Raniganj coal bed methane block," *Journal of the Geological Society of India*, vol 88, no.4, pp. 503-516, 2016.
26. Meng, Y., Tang, D., Xu, H., Li, C., Li, L. and Meng. S. (2014): "Geological controls and coalbed methane production potential evaluation: a case study in Liulin area, eastern Ordos Basin, China,"*Journal of Natural Gas Science and Engineering*, vol 21, pp. 95-111, 2014.
27. Kumar, B., Singh, S. N. (2015): "Analytical studies on the hydraulic performance of chevron type plate heat exchanger," *International Journal of Heat and Technology*, vol 33, no.1, pp.17-24, 2015.
28. Wei, Y. C., Zhang, Q., Wang, A. M., Ren, H. K., Yuan, Y. and Cao, D. Y. (2016): "The influence of the salinity of groundwater in coal measures on low rank coalbed methane in the southern margin of Junggar basin," *Coal Geology & Exploration*, vol 44, no.1, pp.31-37, 2016.
29. Zhang. X. Q. (2015): "Hydraulic characteristics of rational flow shaft spillway," *International Journal of Heat and Technology*, vol 33, no.1, pp.161-166, 2015.
30. Alam, M. S., Islam, T. and Uddin, M. J. (2016): "Mathematical modeling for heat transfer of a micropolar fluid along a permeable stretching/shrinking wedge with heat generation/absorption," *Mathematical Modelling of Engineering Problem*, vol 3, no.1, pp.1-9, 2016.
31. Alaswad, S. and Xiang, Y. (2017): " A review on condition-based maintenance optimization models for stochastically deteriorating system," *Reliability Engineering & System Safety*, vol 157, pp. 54-63, 2017.